Techniques for Including Dielectrics when Extracting Passive Low-Order Models of High Speed Interconnect*

Luca Daniel
University of California, Berkeley
dluca@eecs.berkeley.edu

Alberto Sangiovanni-Vincentelli
Univ. of California, Berkeley
alberto@eecs.berkeley.edu

Jacob White
Massachusetts Institute of Technology
white@mit.edu

ABSTRACT

Interconnect structures including dielectrics can be modeled by an integral equation method using volume currents and surface charges for the conductors, and volume polarization currents and surface charges for the dielectrics. In this paper we describe a mesh analysis approach for computing the discretized currents in both the conductors and the dielectrics. We then show that this fully mesh-based formulation can be cast into a form using provably positive semidefinite matrices, making for easy application of Krylov-subspace based model-reduction schemes to generate accurate guaranteed passive reduced-order models. Several printed circuit board examples are given to demonstrate the effectiveness of the strategy.

1. INTRODUCTION

Dielectric materials are present in almost all modern electronic circuits: from Printed Circuit Boards (PCBs), to packages, Multi-Chips Modules (MCMs), and Integrated Circuits. Dielectrics can significantly affect both the performance and the functionality of electronic circuits. For instance, they can change interconnect delays, as well as the positions of frequency response resonances. Ignoring dielectrics can therefore potentially lead to very inaccurate results both in timing analysis tools and in signal integrity tools.

Integral equation methods have proved to be very effective tools for analyzing on-chip and off-chip interconnect structures, and there are several approaches for including dielectric interfaces in integral formulations. For problems which can be viewed as flat interfaces of infinite extent, such as multilayer printed circuit boards, the dielectric interface conditions can be satisfied by an appropriate choice of Green's function [1, 2, 3, 4, 5]. For general shape or finite-size dielectric bodies, it is possible to "replace" the dielectrics with equivalent fictitious electric and/or magnetic surface currents [6, 7]. General dielectric shapes can also be handled by a volume integral equation (VIE) approach, in which case the polarization currents are introduced in the volume of the dielectrics, and charges are introduced on their surfaces [8, 9].

As the last decade has made clear, detailed electromagnetic analysis is a vastly more effective tool if it can be used to automatically generate accurate circuit-level models of the interconnect. In this paper we show that careful discretization of the VIE method leads to, at least in the low frequency regime, a linear dynamical system with positive semi-definite matrices. This positive-definite result is important because it makes possible the straight-forward application of the Krylov-subspace based guaranteed passive model-order reduction (MOR) techniques [10, 11, 12, 13, 14, 15, 16, 17].

The paper is organized as follows: in Section 2 we summarize Maxwell equations in VIE form. In Section 3, we describe the mesh analysis formulation for dielectrics. In Section 4 we show that the matrices resulting from the VIE full mesh analysis approach can be cast into a positive semidefinite form, hence allowing guaranteed passive low order models extraction. Finally, in Sections 6 and 7 we show the results of our implementation on simple examples of interconnect structures including dielectrics.

2. BACKGROUND

Maxwell equations in Mixed Potential Integral Equation (MPIE) form are as shown in (1)-(4), where V_c and V_d are the union of the conductor and dielectric volumes respectively, $\mathbf{r_c}$ and $\mathbf{r_d}$ are vectors indicating points in V_c and V_d respectively. μ is the magnetic permeability, ε_0 is the permittivity, ε_r is the dielectric relative permittivity, σ_c is the conductivity of the metal, and ω is the angular frequency of the conductor excitation. $\mathbf{J_c}$ is the current density in the conductors. $\mathbf{J_d} = j\omega(\varepsilon - \varepsilon_0)\mathbf{E}$ is the polarization current density in the interior of the dielectrics, and $\mathbf{E}$ is the electric field. The kernel $K(\cdot,\cdot)$ for a full-wave formulation is a frequency dependent function

$$K(\mathbf{r_1},\mathbf{r_2}) = \frac{e^{j\omega\sqrt{\varepsilon_0\mu}|\mathbf{r_1}-\mathbf{r_2}|}}{|\mathbf{r_1}-\mathbf{r_2}|}. \quad (5)$$

When the relevant length scales are much smaller than a wavelength, the above kernel can be approximated with the frequency independent function

$$K(\mathbf{r_1},\mathbf{r_2}) = \frac{1}{|\mathbf{r_1}-\mathbf{r_2}|}. \quad (6)$$

The scalar potentials ϕ_c and ϕ_d, can be related to the surface charge ρ_c and ρ_d, on *both the conductor and dielectric surfaces* as shown in (3)-(4), where S_c is the union of the conductor surfaces, S_d is the union of the dielectric surfaces, $\mathbf{r_{cs}}$ is a vector indicating a point in S_c, and $\mathbf{r_{cs}}$ is a vector indicating a point in S_d. Within each conductor, and within each homogeneous block of dielectric,

$$\nabla \cdot \mathbf{J_c}(\mathbf{r_c}) = 0 \quad (7)$$

$$\nabla \cdot \mathbf{J_d}(\mathbf{r_d}) = 0 \quad (8)$$

*This work was supported by the MARCO Interconnect Focus Center, and by the Semiconductor Research Corporation.
The authors would also like to thank Matt Kamon for useful feedback and discussion.

ICCAD 2001, November 4-8, 2001, San Jose, California, USA.

$$\frac{\mathbf{J_c}(\mathbf{r_c})}{\sigma_c} + j\omega\frac{\mu}{4\pi}\left[\int_{V_c} K(\mathbf{r_c},\mathbf{r_c}')\,\mathbf{J_c}(\mathbf{r_c}')\,d\mathbf{r_c}' + \int_{V_d} K(\mathbf{r_c},\mathbf{r_d}')\,\mathbf{J_d}(\mathbf{r_d}')\,d\mathbf{r_d}'\right] = -\nabla\phi_c \quad (1)$$

$$\frac{\mathbf{J_d}(\mathbf{r_d})}{j\omega(\varepsilon-\varepsilon_0)} + j\omega\frac{\mu}{4\pi}\left[\int_{V_c} K(\mathbf{r_d},\mathbf{r_c}')\,\mathbf{J_c}(\mathbf{r_c}')\,d\mathbf{r_c}' + \int_{V_d} K(\mathbf{r_d},\mathbf{r_d}')\,\mathbf{J_d}(\mathbf{r_d}')\,d\mathbf{r_d}'\right] = -\nabla\phi_d \quad (2)$$

$$\frac{1}{4\pi\varepsilon_0}\left[\int_{S_c} K(\mathbf{r_{cs}},\mathbf{r'_{cs}})\,\rho_c(\mathbf{r'_{cs}})\,d\mathbf{r'_{cs}} + \int_{S_d} K(\mathbf{r_{cs}},\mathbf{r'_{ds}})\,\rho_d(\mathbf{r'_{ds}})\,d\mathbf{r'_{ds}}\right] = \phi_c(\mathbf{r_{cs}}) \quad (3)$$

$$\frac{1}{4\pi\varepsilon_0}\left[\int_{S_c} K(\mathbf{r_{ds}},\mathbf{r'_{cs}})\,\rho_c(\mathbf{r'_{cs}})\,d\mathbf{r'_{cs}} + \int_{S_d} K(\mathbf{r_{ds}},\mathbf{r'_{ds}})\,\rho_d(\mathbf{r'_{ds}})\,d\mathbf{r'_{ds}}\right] = \phi_d(\mathbf{r_{ds}}) \quad (4)$$

for all points $\mathbf{r_c}$ and $\mathbf{r_d}$ in the *interior* of V_c and V_d respectively. In addition, the current normal to the conductor and dielectric surfaces is responsible for the accumulation of surface charge,

$$\hat{\mathbf{n}}\cdot\mathbf{J_c}(\mathbf{r_{cs}}) = j\omega\rho_c(\mathbf{r_{cs}}) \quad (9)$$

$$\hat{\mathbf{n}}\cdot\mathbf{J_d}(\mathbf{r_{ds}}) = j\omega\rho_d(\mathbf{r_{ds}}) \quad (10)$$

where $\hat{\mathbf{n}}$ is the unit normal to S_c and S_d at the points $\mathbf{r_{cs}}$ and $\mathbf{r_{cs}}$ respectively.

The main unknowns, $\mathbf{J_c}$, $\mathbf{J_d}$, ρ_c, and ρ_d can be approximated by a weighted sum of a finite set of basis functions. One classical choice for the basis functions is to cover the surface of each conductor and of each dielectric with *panels*, each of which hold a constant charge density. To model current flow, the interiors of all conductors and dielectrics are divided into a 3-D grid of *filaments*. Fig. 3 shows an example of the 3D volume discretization of a dielectric parallelepiped. Each filament carries a constant current. Other basis functions choices are possible for the interior of the conductors [18].

A Galerkin method [19] can be used to transform the Mixed Potentials Integral Equations (1)-(4) into an algebraic form

$$\begin{bmatrix} R+sL+\frac{1}{s}\begin{bmatrix}0&0\\0&Pol\end{bmatrix} & \begin{bmatrix}0&0\\0&0\end{bmatrix} \\ \begin{bmatrix}0&0\\0&0\end{bmatrix} & P \end{bmatrix} \begin{bmatrix} I_c \\ I_d \\ q_c \\ q_d \end{bmatrix} = \begin{bmatrix} V_c \\ V_d \\ \phi_c \\ \phi_d \end{bmatrix} \quad (11)$$

where I_c, I_d, q_c and q_d are vectors of basis function weights for the conductor currents, dielectric polarization currents, conductor charges and dielectric charges respectively. V_c, V_d, ϕ_C and ϕ_d are the vectors generated by inner products of the basis functions with the potential gradient and with the potential itself. The resistance matrix R, the inductance matrix L and the coefficients of potential matrix P are all derived directly from the Galerkin condition [19],

$$R = \begin{bmatrix} R_c & 0 \\ 0 & 0 \end{bmatrix}, \quad (12)$$

$$L = \begin{bmatrix} L_{cc} & L_{cd} \\ L_{dc} & L_{dd} \end{bmatrix}, \quad (13)$$

$$P = \begin{bmatrix} P_{cc} & P_{cd} \\ P_{dc} & P_{dd} \end{bmatrix}. \quad (14)$$

L and P are frequency dependent when using a full-wave kernel as in (5), and frequency independent when using a quasi-static kernel as in (6). Matrix *Pol* in (11) is a diagonal matrix carrying the polarization coefficients

$$Pol_{i,i} = \frac{l_i}{A_i(\varepsilon-\varepsilon_0)} \quad (15)$$

where l_i and A_i are the length and the cross-sectional area of dielectric filament i respectively.

3. THE MESH FORMULATION

Imposing charge conservation (9)-(10) and current conservation (7)-(8) *on surface and on interior of both conductors and dielectrics* makes it possible to use a mesh analysis approach. As a summary, a complete mesh formulation for structures including both conductors and dielectrics, after the Galerkin transformation can be written simply as:

$$M Z_{cd} M^T I_m = V_{m_s} \quad (16)$$

where I_m are the unknown mesh currents, V_{m_s} is the vector of known mesh voltage sources, non zero only on the rows associated with the external circuit terminals. Z_{cd} is the Galerkin impedance matrix

$$Z_{cd} = \begin{bmatrix} R+sL+\frac{1}{s}\begin{bmatrix}0&0\\0&Pol\end{bmatrix} & 0 \\ 0 & \frac{1}{s}P \end{bmatrix} \quad (17)$$

M is a very sparse mesh analysis matrix,

$$M = [M_{fc} M_d M_{pc} M_{pd}], \quad (18)$$

where submatrices M_{fc} and M_{pc} are the KVL's mesh matrices for the conductors filaments and panels as described in [20]. In a very similar way to [20], we can construct also M_{fd} and M_{pd}, the KVL's mesh matrices for the dielectric filaments and panels. In fact, as for the conductors, dielectric panel charges can be treated as displacement currents flowing on circuit branches to the node at infinity. A set of independent meshes for the three dimensional discretization of the block of dielectric can be found using a minimum spanning tree.

4. PASSIVE MODEL ORDER REDUCTION

In this Section, we will limit ourself to the usage of the quasi-static kernel in (6) which produces frequency independent L and P matrices in (13) and (14). The technique to handle dielectrics in [21] uses a similar quasi-static assumption, and seems more advantageous requiring fewer unknowns. However, not only magnetic coupling between conductive and polarization currents are neglected by that formulation, but also the matrices used in that formulation are not in the form required for Krylov-subspace based passive model-reduction schemes [10]. In this Section, we show instead an easy way to cast our mesh analysis approach into a form suitable for passive reduced order modeling.

Let us choose as state vector for a linear system representation:

$$x = \begin{bmatrix} I_m & Q_{cs} & Q_{ds} & Q_{dv} \end{bmatrix}^T \quad (20)$$

In view of this choice, we can rewrite (16) as shown in (19) on next page, where

$$[Q_{cs}\,Q_{ds}\,Q_{dv}]^T = [M_{pc}\,M_{pd}\,M_{fd}]^T \frac{I_m}{s}. \quad (21)$$

$$[M_{fc}M_{fd}]\,[R+sL]\,[M_{fc}M_{fd}]^T I_m \;+\; [M_{pc}M_{pd}]\,P\,[Q_{cs}Q_{ds}]^T \;+\; M_{fd}\,[Pol]\,Q_{dv} = V_{m_s} \tag{19}$$

Or finally in linear system terms:

$$\hat{L}\frac{dx}{dt} = -\hat{R}x(t) + Bu(t) \tag{22}$$

$$y(t) = Cx(t) \tag{23}$$

where matrices $\hat{L}$ and $\hat{R}$ are defined as

$$\hat{L} = \begin{bmatrix} [M_{fc}M_{fd}]\,L\,[M_{fc}M_{fd}]^T & 0 & 0 \\ 0 & P^T & 0 \\ 0 & 0 & [Pol]^T \end{bmatrix} \tag{24}$$

$$\hat{R} = \begin{bmatrix} [M_{fc}M_{fd}]\,R\,[M_{fc}M_{fd}]^T & [M_{pc}M_{pd}]P & M_{fd}[Pol] \\ -P^T[M_{pc}M_{pd}]^T & 0 & 0 \\ -[Pol]^T M_{fd}^T & 0 & 0 \end{bmatrix} \tag{25}$$

Vector $u(t)$ contains the excitation voltage sources, $Bu(t) = V_{ms}$. Vector $y(t)$ contains the observed output currents, derived through matrix C from the mesh currents I_m in the state vector $x(t)$.

THEOREM 1. *Matrices $\hat{L}$ and $\hat{R}$ in (24) and (25) are positive semidefinite.*

PROOF. The polarization matrix $[Pol]$ is diagonal with positive coefficients, hence it is positive semidefinite. When using a Galerkin technique [19], the coefficient of potential matrix P in (14) and the inductance matrix L in (13), are both positive semidefinite. The matrix $[M_{fc}M_{fd}]\,L\,[M_{fc}M_{fd}]^T$ is then also positive semidefinite. Since all the three blocks of the block-diagonal matrix $\hat{L}$ in (24) are positive semidefinite, $\hat{L}$ is positive semidefinite. This concludes the first part of the proof.

To prove that $\hat{R}$ in (25) is positive semidefinite let us calculate:

$$\hat{R}+\hat{R^T} = \begin{bmatrix} 2\,[M_{fc}M_{fd}]\,R\,[M_{fc}M_{fd}]^T & 0 & 0 \\ 0 & 0 & 0 \\ 0 & 0 & 0 \end{bmatrix} \tag{26}$$

The resistance matrix R is positive semidefinite, hence the submatrix $2\,[M_{fc}M_{fd}]R[M_{fc}M_{fd}]^T$ is positive semidefinite and so is $\hat{R}+\hat{R^T}$. Since $x^T(\hat{R}+\hat{R^T})x = 2x^T\hat{R}x$, we can then finally conclude that $\hat{R}$ is positive semidefinite. □

OBSERVATION 1. *When modeling the input impedances and the transfer functions of a 3D structure, we apply input voltages at some ports, and we measure the resulting currents on the same set of ports, hence we are choosing $C = B^T$ in eq (22) and (23).*

OBSERVATION 2. *From Theorem 1 and from Observation 1, one can conclude that the formulation in (22)-(25) satisfies to the conditions for guaranteed passive Krylov subspace based model reduction in [10].*

5. SUMMARY OF OUR PROCEDURE

We summarize here briefly for the convenience of the reader our entire proposed procedure in its final form:

1. First, we discretize both the volumes and the surfaces of the conductors and dielectrics. An example is shown in Fig. 3.

2. We use a standard Galerkin technique [19] to construct matrices R, L, P, Pol in eq.(12) to (15).

3. A mesh analysis approach is used to construct the sparse KVL's matrices M_{fc}, M_{fd}, M_{pc}, and M_{pd} in (18). More details on how to handle conductors are in [20]. For the dielectrics, we use a minimum spanning tree to find a set of independent meshes.

4. A Krylov subspace based model reduction algorithm such as [10] is then used to produce reduced order linear system models. At each step of the algorithm the quantity $[\hat{R}+s_0\hat{L}]^{-1}\hat{L}\,v$, could be computed using fast matrix vector products and Krylov subspace iterative methods.

5. The reduced order model is then used to obtain a plot of the frequency response as in Fig. 1, and Fig. 4 or to produce an equivalent SPICE circuit for a time domain simulation including the non-linear circuitry.

The overall complexity of this procedure is $O(N_m\,Nlog(N))$, where N_m is the total number of moments matched by the model reduction algorithm at all frequency expansion points. N is the size of the original full linear system model in (22)-(23), or about the number of basis functions used in the volume and surface discretization.

6. A TRANSMISSION LINE EXAMPLE

Two PCB traces are considered in this example in a transmission line configuration. Traces are located on opposite sides of a dielectric substrate, and shorted at one end. Fig 1 shows the frequency response of such transmission line structure. In Fig 1 we also show the response of the calculated reduced order model.

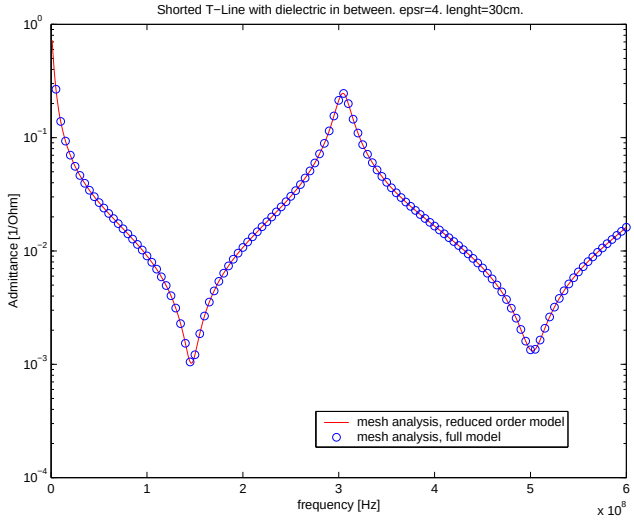

Figure 1: Reduce order modeling of a shorted PCB transmission line. Traces' dimensions are 250μm x 35μm x 30cm. A 100μm thick dielectric layer ($\varepsilon_r = 4$) is present between the two traces. The continuous line is the admittance vs. frequency of the calculated reduced model. The circles are the response of the original system.

At the frequencies where the frequency independent kernel in (6) yields accurate results, it may also be reasonable to neglect magnetic coupling between conductors and dielectric polarization currents. However there are cases where even with a non-fullwave

kernel one might observe some effects of the magnetic coupling between dielectric polarization currents and conductors. One of such cases is illustrated in Fig. 2. A via is located in proximity of the shorted PCB transmission line. The line is then excited at a frequency close to the first quarter-wavelength resonance. In this situation most of the current closes its path through the dielectric layer in the form of polarization currents. If a nearby via corresponds to a quiet victim line, some coupling can be observed between the vertical polarization currents and the via.

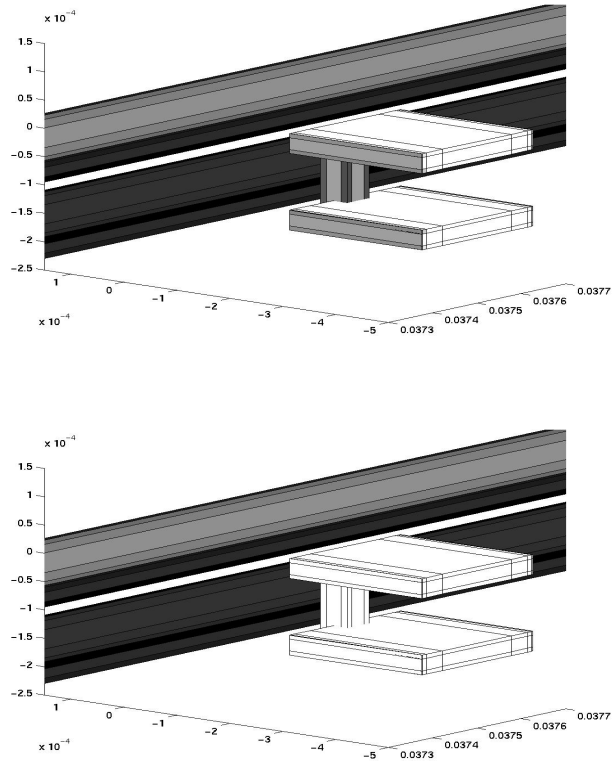

Figure 2: Via located near a PCB transmission line. In this picture we do not show the dielectric layer which is located between the two dark PCB transmission line traces. Shadings correspond to current density amplitudes. On top we show the current densities corresponding to the case where magnetic coupling between polarization currents and conductors is accounted for. On the bottom we show the same example but setting $L_{cd} = 0$, $L_{dc} = 0$ and $L_{dd} = 0$ in (13) which corresponds to neglecting magnetic coupling between polarization currents and conductors.

7. MCM INTERCONNECT EXAMPLE

In a second example, we have applied our technique to analyzing two wires of an interconnect bus on an Multi-Chip Module (MCM), as shown in Fig. 3. A dielectric layer ($\varepsilon_r = 4$) is present underneath the traces and the chips. In Fig. 4 we show the frequency response of the two interconnects when shorted on one side and driven on the other. We show the frequency response with and without the dielectric substrate. A significant difference in the resonance position can be observed. Fig. 3 shows the polarization volume currents at the first resonance $f = 3$ GHz. In Fig. 4 we compare the reduced

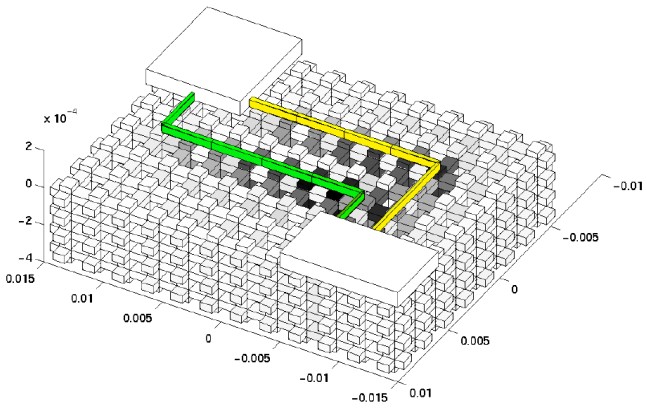

Figure 3: Two traces part of an MCM interconnect system (figure above). A dielectric layer $\varepsilon_r = 4$ is present underneath the traces and the chips. The figure below shows the volume polarization currents inside the dielectric layer at the 3 GHz resonance. For visualization purposes, the axes in this picture are not "to-scale". Traces are 2cm long, 4mm far apart, 250μm wide and 40μm thick.

order model to the full model for the case when the dielectric substrate is present. The reduced order model has been built matching four moments around each of the following expansion points: $s_1 = j2\pi \cdot 100$ KHz, $s_2 = j2\pi \cdot 3$ GHz, and $s_3 = j2\pi \cdot 6$ GHz. In order to include also the point $s_0 = 0$ among the other expansion points, a non-singular $\hat{R}$ in (25) would be necessary. It can been shown [22] that a matrix of the form such as in (25) is non-singular under the condition that there are no cut-sets of only capacitors. Unfortunately, each node in our dielectric discretization is such a cut-set when dielectric losses are negligible. Therefore, for lossless dielectrics the point $s_0 = 0$ cannot be included in the multipoint expansion algorithm, and a non-zero low frequency expansion point is used instead. From our experiments, we have observed that this expansion point restriction is not interfering with accuracy. For instance in this particular example, the zero frequency behavior of the structure has been accurately captured as shown in Fig. 5, which is a magnified view of the low frequency part of the plot in Fig. 4,

8. CONCLUSIONS

In this paper we described applying the mesh analysis approach to solving for the discretized currents and charges in a VIE formulation. We showed that the approach leads to a system with provably positive semidefinite matrices, making for easy application of Krylov-subspace based model-reduction schemes to generate accurate guaranteed passive reduced-order models. Several printed circuit board examples demonstrated the effectiveness of the strategy.

Arguably, it is tempting to assume that the VIE approach is a step backward, as it involves discretizing volumes instead of surfaces. However, volume integral equation methods are used for magnetic analysis of conductor problems, because conductors occupy a vanishingly small region of the problem domain. The same vanishingly small occupancy argument can be made for dielectrics as well. In addition, since polarization currents are not "outputs", it

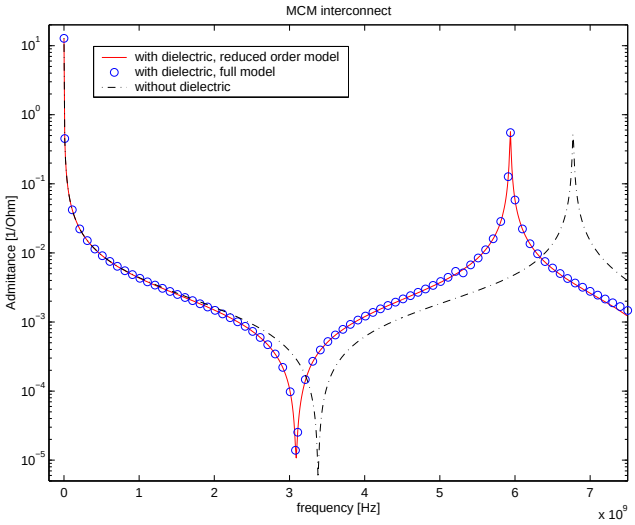

Figure 4: Admittance vs. frequency for the two traces in Fig. 3.

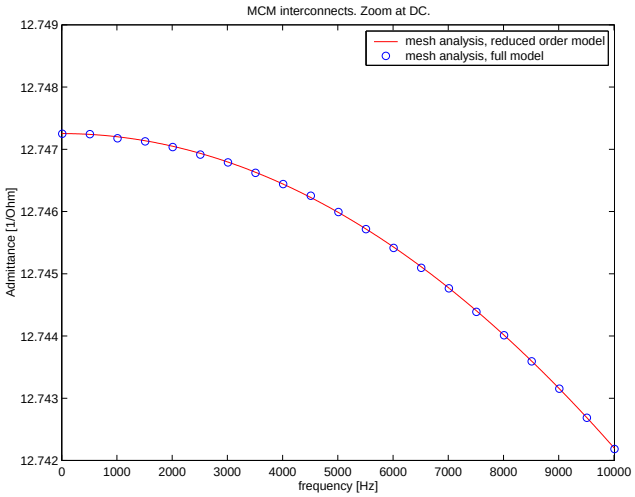

Figure 5: Magnified view of the low frequency part of the plot in Fig. 4, to verify that the reduced model (continuous line) captures correctly the DC behavior of the original system (circles).

might be possible to align them with a regular grid. Such an alignment might improve the performance of fast solvers, such as the Conjugate Gradient FFT (CGFFT) [23] or Precorrected-FFT [24] methods. This is an important consideration since such solvers are required when using any integral formulation on models with complicated geometries.

9. REFERENCES

[1] Y. L. Chow, J. J. Yang, D. G. Fang, and G. E. Howard. A closed-form spatial green's function for the thick microstrip substrate. *IEEE Trans. on Microwave Theory and Techniques*, 39(3):588–592, March 1991.

[2] M. I. Aksun and R. Mittra. Derivation of closed-form green's functions for a general microstrip geometry. *IEEE Trans. on Microwave Theory and Techniques*, 40(11):2055–62, November 1992.

[3] K. A. Michalski and J. R. Mosig. Multilayered media green's functions in integral equation formulations. *IEEE Trans. on Antennas and Propagation*, 45(3):508–519, March 1997.

[4] J. Zhao, W. W. M. Dai, S. Kapur, and D. E. Long. Efficient three-dimensional extraction based on static and full-wave layered green's functions. In *Proceedings of the Design Automation Conference*, pages 224–229, 1998.

[5] A. C. Cangellaris and V. Okhmatovsky. New closed-form electromagnetic green's functions in layered media. In *IEEE MTT-S International Microwave Symposium*, pages 1065–8, June 2000.

[6] A. W. Glisson. An integral equation for electromagnetic scattering from homogeneous dielectric bodies. *IEEE Trans. on Antennas and Propagation*, AP-32(2):173–175, February 1984.

[7] D. R. Swatek and Ioan R. Ciric. Single source integral equation for wave scattering by multiply-connected dielectric cylinders. *IEEE Trans. on Magnetics*, 32(3):878–881, May 1996.

[8] A. E. Ruehli and H. Heeb. Circuit models for three-dimensional geometries including dielectrics. *IEEE Trans. on Microwave Theory and Techniques*, 40:1507–1516, July 1992.

[9] T. K. Sarkar and E. Arvas. An integral equation approach to the analysis of finite microstrip antennas: Volume/surface formulation. *IEEE Trans. on Antennas and Propagation*, 38(3):305–312, March 1990.

[10] A. Odabasioglu, M. Celik, and L. T. Pileggi. Prima: Passive reduced-order interconnect macromodeling algorithm. *IEEE Trans. on Computer-Aided Design of Integrated Circuits and Systems*, 17(8):645–54, August 1998.

[11] P. Feldmann and R. W. Freund. Reduced-order modeling of large linear subcircuits via a block lanczos algorithm. In *Proceedings of the Design Automation Conference*, pages 474–479, June 1995.

[12] K. J. Kerns, I. L. Wemple, and A. T. Yang. Stable and efficient reduction of substrate model networks using congruence transforms. In *IEEE/ACM Internat. Conf. on Computer-Aided Design*, pages 207–214, November 1995.

[13] E. J. Grimme. *Krylov projection methods for model reduction*. PhD Thesis, Univ. of Illinois at Urbana-Champaign, 1997.

[14] I. M. Elfadel and D. D. Ling. A block arnoldi algorithm for multipoint passive model-order reduction of multiport rlc networks. *IEEE/ACM Internat. Conf. on Computer-Aided Design*, November 1997.

[15] L. M. Silveira, M. Kamon, I. Elfadel, and J. White. Coordinate-transformed arnoldi algorithm for generating guarantee stable reduced-order models of rlc. *Computer Methods in Applied Mechanics and Engineering*, 169(3-4):377–89, February 1999.

[16] J. E. Bracken, D. K. Sun, and Z. Cendes. Characterization of electromagnetic devices via reduced-order models. *Computer Methods in Applied Mechanics and Engineering*, 169(3-4):311–330, February 1999.

[17] A. C. Cangellaris and L. Zhao. Passive reduced-order modeling of electromagnetic systems. *Computer Methods in Applied Mechanics and Engineering*, 169(3-4):345–358, February 1999.

[18] L. Daniel, A. Sangiovanni-Vincentelli, and J. White. Conduction modes basis functions for efficient electromagnetic analysis of on-chip and off-chip interconnect. In *Proceedings of the Design Automation Conference*, June 2001.

[19] R. F. Harrington. *Field Computation by Moment Methods*. MacMillan, 1968.

[20] M. Kamon, N. Marques, L. M. Silveira, and J. White. Automatic generation of accurate circuit models. *IEEE Trans. on Comp., Packaging, and Manufact. Tech.*, August 1998.

[21] K. Nabors and J. White. Fastcap: a multipole accelerated 3-d capacitance extraction program. *IEEE Trans. on Computer-Aided Design of Integrated Circuits and Systems*, 10(11):1447–59, November 1991.

[22] M. Kamon. *Fast parasitic extraction and simulation of three-dimensional interconnect via quasistatic analysis*. PhD Thesis, Massachusetts Institute of Technology, 1998.

[23] B. G. Salman and A. McCowen. A comparative study of the computation of near-field scattering from resonant dielectric/pec scatterers. *IEEE Trans. on Magnetics*, 32(3):866–9, May 1996.

[24] J. R. Phillips and J. White. A precorrected-fft method for electrostatic analysis of complicated 3-d structures. *IEEE Trans. on Computer-Aided Design of Integrated Circuits and Systems*, 16(10):1059–1072, October 1997.